Heat and Mass Transfer Enhancement in Unsaturated Porous Packed beds subjected to Electrohydrodynamics (EHD)

*Chainarong CHAKTRANOND[1], Phadungsak RATANADECHO[1]
[1]*Department of Mechanical Engineering, Faculty of Engineering, Thammasat University, Rangsit Campus, Khlong Luang, Pathumthani 12121, Thailand*
Corresponding author: Chainarong CHAKTRANOND E-mail: cchainar@engr.tu.ac.th

Keywords: Drying, Heat and mass transfer, Electrohydrodynamics

ABSTRACT

Enhancement of heat and mass transfer in a convective drying of single- and double-layer porous packed bed subjected to electric fields is experimentally investigated and analyzed in this paper. In addition, effect of electrical voltage, porosity, and layer structure on drying behaviors in the packed beds composed of glass beads, water and air are examined. Glass beads of 0.125 and 0.38 mm in diameters are employed in the packed beds. Velocity of hot air is about 0.33 m/s and temperature is controlled at 60^{O}C. Electric fields are applied in the range of 0 - 15 kV. Enhancement of heat and mass transfer is revealed through measuring the temperature and weight loss of moisture content of the packed beds. The results show that the convective heat transfer coefficient and drying rate are enhanced considerably with influence of Corona wind on flow above the packed beds. In addition, arrangement of the glass-bead-layered structure greatly affects on the temperature distribution and rate of moisture content in packed bed. An increase in temperature due to the capillary pressure difference in the double-layered packed bed is more pronounced comparing to that in the single layer bed. Moreover, in the double-layered cases, the drying rate of fine-coarse packed bed is much higher than that of coarse-fine packed bed.

INTRODUCTION

The application of drying techniques for many processes, such as chemical, pharmaceuticals, and agriculture, have been considered for many years. Due to the simultaneous heat and mass transfer taking place during the process, drying is one of most complicated phenomena. In addition, it is not clearly understood.

A conventional drying method with hot-air flow is widely used in agricultural industries for removing the moisture content from products. However, its drying period is long, resulting in large energy consumption. In order to improve drying rate, many researchers have paid much attention in development of hot-air drying cooperating with the other methods, e.g., microwave [1-3], infrared [4, 5], and electric fields [6]. In order to increase removing the moisture within material, microwave irradiation penetrates in the bulk of the material, and creates a heat source at a certain location. To heat the surface region, infrared radiation is transmitted through water at a short wavelength, while it is absorbed on the surface at a long wave length [7]. This drying is suitable to dry thin layers of material with large surface exposed to radiation. In order to enhance the removal of water from the porous material surface, Chaktranond et al. [6] applied the electric fields on the hot-air flow. They report that the effect of the corona wind conducted by electric fields enhances the temperature and drying rate of porous packed bed considerably.

To get more understanding in the mechanisms of drying in porous materials, this study aim to experimentally investigate and analyze the transfer of heat and mass within single- and double layer porous packed bed subjects to the influence of hot-air flow and electric fields. In addition, effects of porosity and layer structure are reported.

CONCEPT AND EQUATIONS

Corona wind

Schematic of heat-and-mass transfer enhancement with utilizing electrohydrodynamics (EHD) is shown in Fig. 1. When hot-air flow exposed to electric fields, it gives rise to an electrically induced secondary flow, so-called Corona wind. With EHD, flow above packed bed is circulated and is mingled together. This reduces the influence of boundary layer on the packed-bed surface. In addition, it causes moisture on surface to be substantially removed into the air flow, while heat is transfered into the packed bed. Consequently, the rate of moisture removal is enhanced.

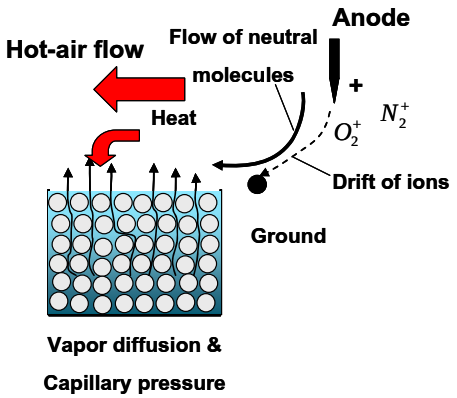

Fig. 1 Schematic of enhancement of heat and mass transfer with corona wind [6].

Drying equations

Water saturation of a porous medium with respect to a particular fluid is defined as

$$S = \frac{Volume\ of\ \ fluid}{Total\ volume\ of\ voids} = \frac{V_{water}}{V_{void}} \qquad (1).$$

Moisture content in porous material is the ratio of total mass of water to total mass of dry solid, i.e.

$$X = \frac{M_{water}}{M_{solid}} \quad (2).$$

Eq. (2) can be written in term of water saturation (S), and it is

$$X = \frac{\phi \rho_{water}}{(1-\phi)\rho_{solid}} S \quad (3),$$

where ϕ is porosity and ρ is density.

From Fourier's law, heat flux through porous material is computed by

$$q = -\lambda_{eff} \nabla T \quad (4),$$

where λ_{eff} is the effective thermal conductivity, and ∇T is temperature gradient in packed bed. In addition, it is assumed to be a function of water saturation. It is defined as [3]

$$\lambda_{eff} = \frac{0.8}{1+3.7e^{-5.95S}} \quad (5).$$

Exchange of energy at surface of packed bed exposed to air flow can be calculated by

$$-\lambda_{eff} \frac{\partial T}{\partial z} = h_c (T_s - T_{air}) + \dot{m}_{water} h_v \quad (6),$$

where h_c is convective heat transfer coefficient, $\dot{m}_{water}$ is volumetric evaporation rate, h_v is latent heat of vaporization, T_s and T_{air} are temperature at surface and of air, respectively.

The relationship between the capillary pressure and the water saturation is defines by using Leverett functions $J(S_e)$ [2, 3],

$$p_c = p_{gas} - p_{liquid} = \frac{\sigma}{\sqrt{K/\phi}} J(S_e) \quad (7),$$

where p_{gas} and p_{liquid} are pressure of gas and liquid phases, respectively, S_e is the effective water saturation associated with the irreducible water saturation, and σ is surface tension.

EXPERIMENTAL SETUP

Figure 2 shows the schematic diagram of experimental setup. The tested rig is an open system. The wind tunnel opens on one side and hot air is blown into the ambient. Air is supplied from a blower and temperature of air is increased by a hot-air generator, which is connected to the rig. In order to control temperature of hot air, a thermocouple sensor (TC) is placed in front of the test section, which has the dimensions of 15×15 cm^2. The high voltage power supply (LEYBOLD 521721) is used to generate an electrical field in the test section.

Positions of electrodes are shown in Fig. 3. Electrode wires comprise of four positive discharge and one ground electrodes. The discharge electrodes made of copper wires are suspended from the top wall and placed in the front of packed bed. Diameter of each copper electrode is 0.025 mm and the spacing between each wire is 26 mm. Ground electrode is also made of copper wire, but suspended horizontally across the test section. The porous packed bed used in this study is composed of glass beads, water and air. The container of glass beads is made of acrylic plate with a thickness of 0.5 mm. In addition, the dimensions are 3.5 cm wide, 12 cm long and 6 cm high. Moreover, to control heat transfer from hot air towards only the upper surface of packed bed, other sides are insulated by rubber sheet. In order to investigate the heat transfer within the packed bed, three fiber optic wires (LUXTRON Fluroptic Thermometer, Model 790, Santa Clara, Canada, accurate to ±0.5^{O}C) are placed in the middle point of the lines of z = 0, 2, and 4 cm, which are measured from the surface of the packed bed.

Figure 4 shows the configuration of the double-layer packed beds. For the single layer, packed bed is filled with a size of glass bead. While in the double layer, packed bed is filled with two different sizes of glass bead. To define the double-layer cases, fine bead layer being on top of coarse bead layer is defined as the F–C case, and the opposite is defined as the C–F case. Additionally, both layers have a same thickness.

In experiments, the maximum electrical voltage is tested to make sure that a breakdown voltage will not occur. The diameters of glass beads are 0.125 mm for fine beads and 0.38 mm for coarse beads. The details of testing conditions and characteristics of water transport in porous media are shown in Table 1 and 2, respectively.

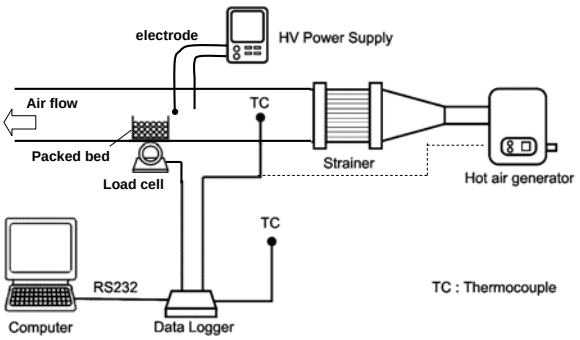

Fig. 2 Schematic diagram of experimental setup.

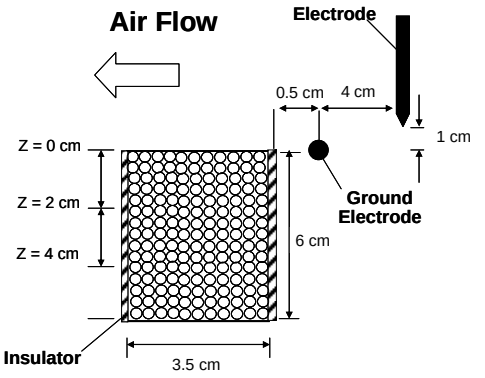

Fig. 3 Dimensions of packed bed, locations of electrodes and temperature measurement.

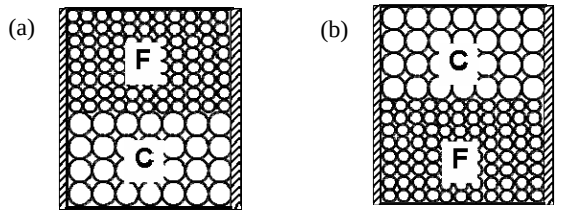

Fig. 4 Configuration of double-layer packed bed: (a) F – C case, and (b) C – F case.

Table 1 Testing conditions

Condition	Symbol	Value
Initial moisture	$X_{db,i}$	22 – 38% db
Drying temperature	T	50 – 60^{O}C
Ambient temperature	T_a	25^{O}C
Mean air velocity	U_b	0.33 m/s
Applied voltage	V	0, 10, 15 kV
Drying time	t	24 – 48 hr
Glass bead	d	0.125, 0.38 mm

Table 2 Characteristics of water transport in porous media.

Diameter, d (mm)	Porosity, ϕ	Permeability, K (m^2)
0.125	~ 0.385	$\sim 8.41 \times 10^{-12}$
0.38	~ 0.371	$\sim 3.52 \times 10^{-11}$

RESULTS AND DISCUSSIONS

Flow visualization

In order to observe the motion of flow subjected to the electric fields, this study utilizes an incense smoke technique. A spot light of 500 W is placed at the outlet of channel, and the light direction is opposite to the flow direction. Due to high speed of flow, the bulk mean velocity is reduced to 0.1 m/s. In addition, the motion of flow is continuously captured by a digital video camera recorder (SONY DCR-PC108/ PC109E).

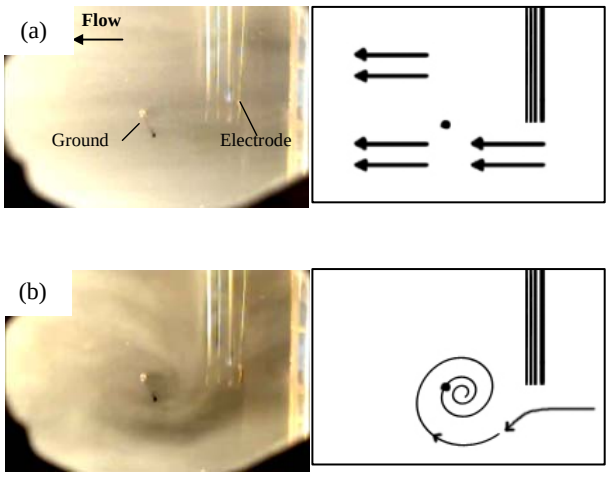

Fig. 5 Motion of air flow at 0.1 m/s: (a) without electric fields, and (b) with electric fields at V = 10 kV.

As shown in Fig. 5, under the influence of EHD, the air flow neighboring electrodes is induced by electric fields, and is circulated around ground electrode. In addition, strength of vortex varies with the magnitude of electrical voltage applied.

In measuring the temperature in the packed bed, it is assumed that temperature is in state of thermodynamic equilibrium, thus temperatures of all phases, i.e. solid, liquid, and gas, are same. The average temperature of hot air, which is measured behind packed bed, approximately is 60^{O}C. Reynolds number, (Re = $\rho U_b D_h/\mu$, where ρ is density of air, μ is viscosity of air, and D_h is hydraulic diameter) of air flow is 3049.

Single-layer packed bed

Figure 6 and 7 show the influence of EHD on temperature in packed bed with 0.125-mm bead at z = 0 and 4 cm, respectively. Clearly, when electric fields are applied, the temperature in packed bed increases, In addition, higher voltage applied causes higher temperature. Moreover, EHD influences the surface temperature more than the inside. This is because EHD induces secondary flow, so-called Corona wind. The effect of this Corona wind circulating above packed bed enhances the mass transfer, and destabilizes the boundary layer on the surface. Consequently, convective heat transfer coefficient is enhanced, and then heat from hot-air flow can substantially transfers into the packed bed. Therefore, the temperature of the cases with EHD is higher than that of the cases without EHD.

In this study, the increase in convective heat transfer due to EHD is defined as the ratio convective heat transfer coefficient with EHD to convective heat transfer coefficient with free air, i.e. $h_{c.EHD} / h_{c,\,free}$, and the results are shown in Fig. 8. In warm-up period, this ratio increases rapidly. In addition, in constant rate of drying period (constant surface temperature), the ratios are about 2 and 3 for cases with V = 10 and 15 kV, respectively.

As shown in Fig. 9, with voltage applied, water saturation in packed bed is much more reduced, resulting in enhancement of mass transfer. In constant rate of drying period, the drying rate with EHD is approximately 2 times higher than that with hot-air flow only, as shown in Fig. 10.

Heat transfer behavior in packed bed with big bead (0.38 mm) is shown in Fig. 11. Without EHD, temperature difference between at surface and inside is not much different. While with voltage applied, temperature difference is clearly observed. Moreover, they are higher than those without voltage applied.

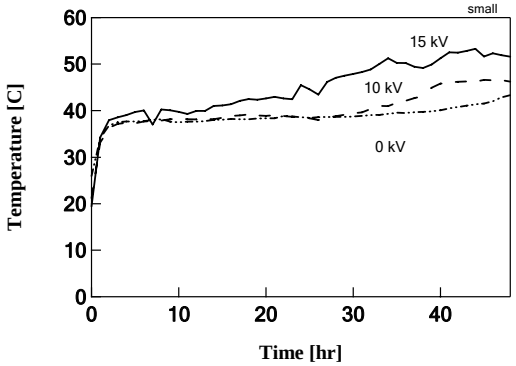

Fig. 6 Surface temperature (z = 0 cm) of packed bed with 0.125-mm bead in various voltages.

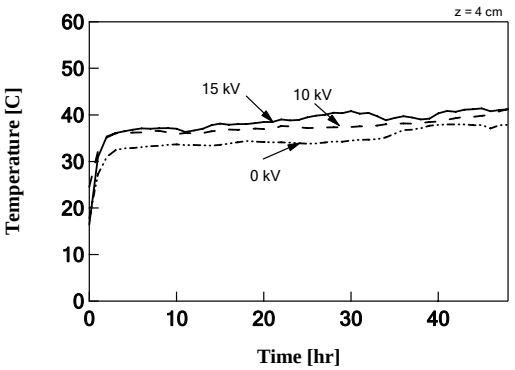

Fig. 7 Temperature of packed bed with 0.125-mm bead at z = 4 cm.

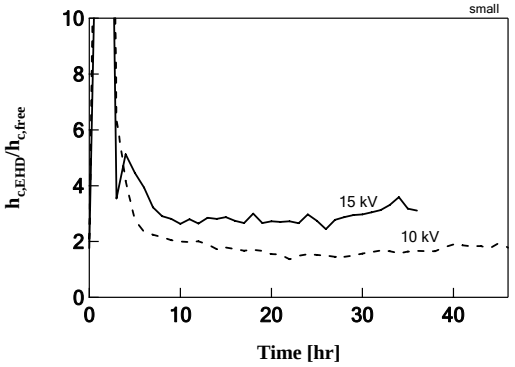

Fig. 8 Enhancement of heat transfer coefficient in case of packed bed with 0.125-mm bead.

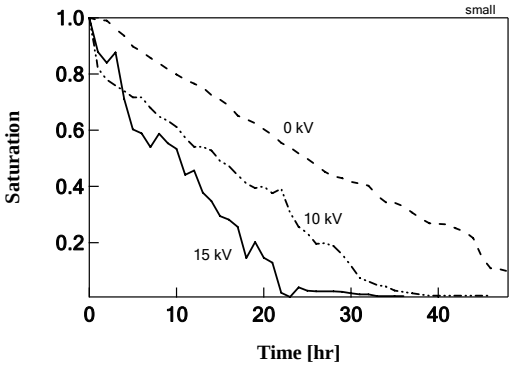

Fig. 9 Comparison on water saturation of packed bed with 0.125-mm bead in various voltages**.**

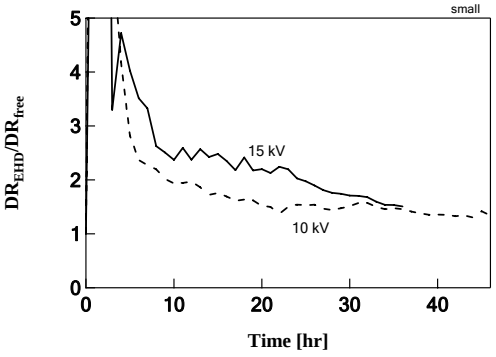

Fig. 10 Enhancement of rate of mass transfer in case of packed bed with 0.125-mm bead.

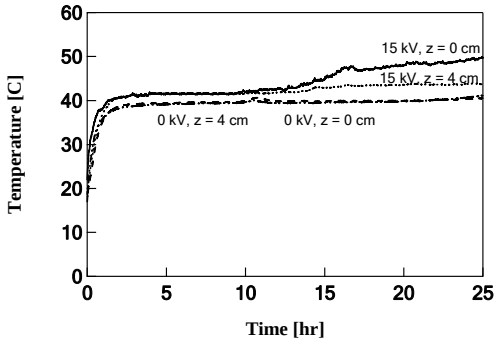

Fig. 11 Temperature of packed bead with 0.38-mm bead in various voltages at z = 0 and 4 cm.

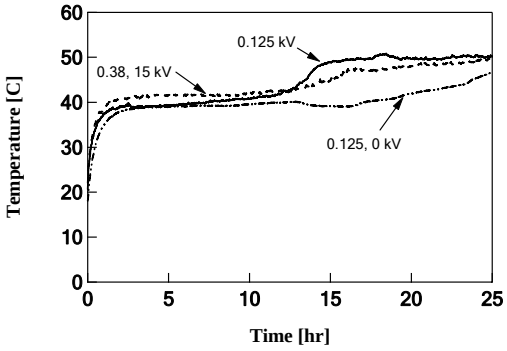

Fig. 12 Comparison on surface temperature (z = 0 cm) of packed bead with 0.38-mm and 0.125-mm beads.

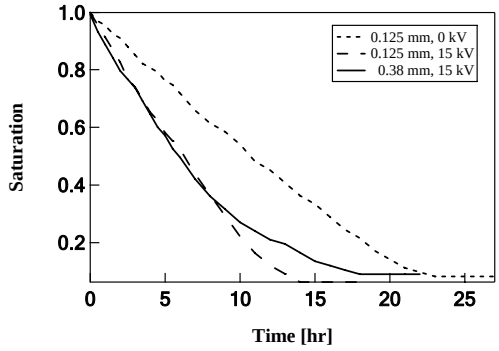

Fig. 13 Comparison on saturation in packed bead with different glass bead sizes.

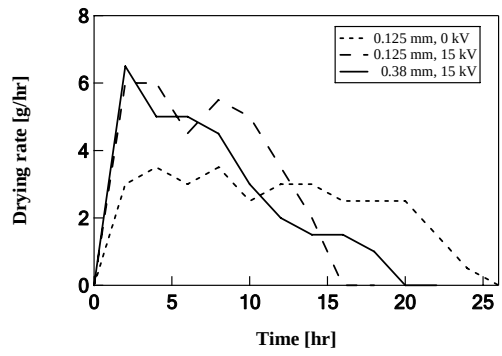

Fig. 14 Comparison on drying rate in packed bead with different glass bead sizes.

Influence of porosity or glass bead size on heat and mass transfer are shown in Fig. 12 - 14. After a constant rate of drying period, surface temperature in packed bed with small bead (0.125 mm) rapidly increases, while temperature in the case of packed bed with big beads (0.38 mm) gradually increases. It is shown in Fig. 13 that high rate of drying in case of small bead remains longer than that in case of big bead. This is because effect of capillary pressure in packed bed with small beads is greater than that with big beads. From Eq. (7), if $(\sigma J(S_e))_{\text{fine}} \sim (\sigma J(S_e))_{\text{coarse}}$ then $p_{c,\text{fine}} > p_{c,\text{coarse}}$. It means that in the case of same saturation, a smaller particle size corresponds to a higher capillary pressure. Therefore, more moisture is transferred from inside packed bed to the surface.

Double-layer packed bead

In order to investigate the temperature on the interface layer, in case of double-layer packed, one more fiber optic wire is placed at z = 3 cm.

Figure 15 and 16 show temperature in the packed bed of F-C case. It is observed that in the warm-up period, all temperatures in this packed bed rise up steadily. Later, they remain constant, as surface temperature of packed bed is lowest. Until a certain time, the temperature on surface rises rapidly, and is higher than the other layers. This is because of the effect of capillary pressure difference. As addressed above, packed bed with small bead provides the capillary pressure (p_c) higher than that with big bead. In the initial period, if both layers have same amount of saturation, then difference of capillary pressure will occur. Therefore, effect of capillary action in the fine bead layer (upper layer) will induce the moisture to flow from the coarse bead layer (lower layer) to its layer. This causes void in the lower layer to be filled with more the vapor phase. Therefore, with a same heat flux, temperature in lower layer becomes higher. As moisture evaporating process proceeds, temperatures of porous packed are constant, where heat is used for changing phase. Until a certain time, the surface becomes dry; heat will mainly transfer by conduction. Consequently, temperature in the upper layer rises up again when drying zone is initiated, and the temperature of surface layer is higher than the other layers.

Figure 17 and 18 show temperature variations in the case that coarse beads overlay fine beads. Unlike F-C case, without electric fields applied, the temperature on the surface layer is highest. While with electric fields applied, temperature on the surface becomes lowest during the early period. In addition, temperature is higher when electrical voltage increases. Even though when electrical voltages are applied, the results from the C-F case and from F-C case are similar. Temperatures in C-F cases are still low. This is because moisture in the coarse layer (upper layer) slowly transfers to the surface, and this effect retards the moisture transfer from the lower layer to the upper.

It is evident in Fig. 19 that the moisture removal in C-F cases is much lower than that in F-C cases. With the influence of EHD, the drying rate can be increased. In addition, rate of drying of F-C cases is about 3.13 – 3.67 times higher than that of C-F case. Moreover, with voltage applied, the drying rate is improved up to about 1.5 – 1.97 times.

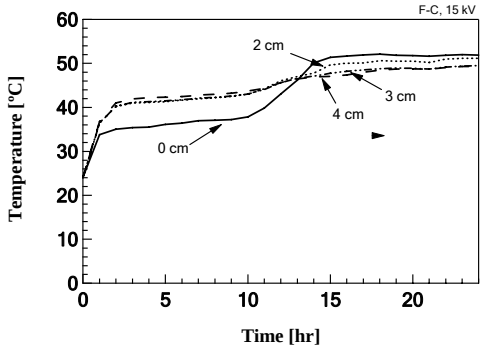

Fig. 15 Temperature in F-C packed bed when V = 15 kV.

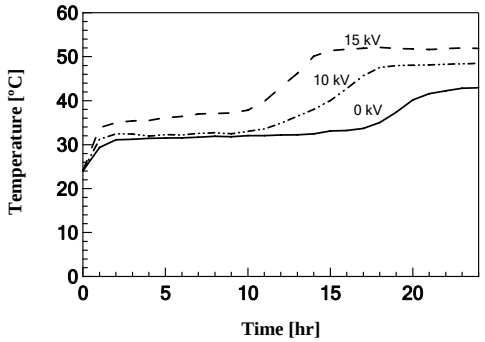

Fig. 16 Temperature at z = 0 cm in F-C packed bed in various voltages.

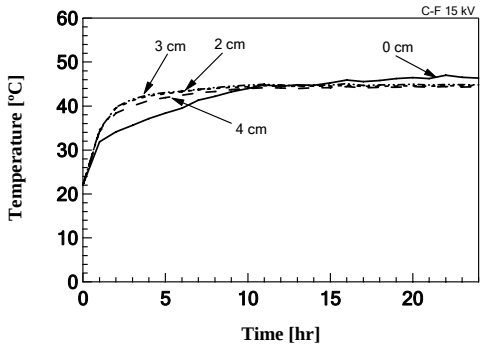

Fig. 17 Temperature in C-F packed bed when V = 15 kV.

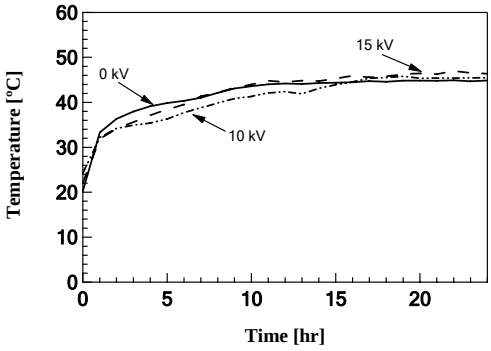

Fig. 18 Temperature at z = 0 cm in C-F packed bed in various voltages.

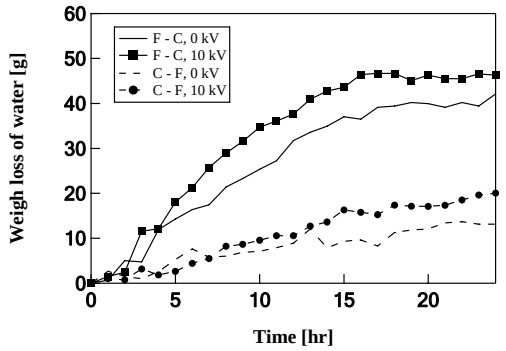

Fig. 19 Comparison on weight loss of water from packed bed in various cases.

CONCLUSIONS

Effects of electrical voltage, porosity, and porous structure on heat and mass transfer in the porous packed beds subjected to hot-air flow and electric field are analyzed through experimental results.

Corona wind circulating above packed bed augments the convective heat transfer coefficient and evaporation rate on the packed bed surface exposed to hot-air flow, resulting in enhancement of heat and mass transfer in packed bed. In addition, the augmentation depends on the magnitude of voltage applied, and porosity of packed bed. Larger porosity provides higher the capillary pressure.

Due to effect of capillary pressure difference, heat and mass transfer in double-layer packed bed exhibit behaviors different than that in single one. With retarding of moisture motions in the upper layer of C-F cases, moisture in the lower layer does move much towards the upper layers, resulting in low temperature. In contrast, F-C cases conduct moisture in the lower layers towards the upper layers better. With voltage applied, the drying rate is improved about 1.5 – 1.97 times. In addition, the drying rate of F-C cases is about 3.13 – 3.67 times higher than that of C-F cases.

ACKNOWLEDGEMENTS

This work was supported through the research fund by Thailand Research Fund (TRF).

REFERENCES

1. Gori, F., Gentili, G., and Matini, L. (1987). Microwave heating of porous media. ASME J. Heat Transfer, 109, pp. 522-525.
2. Ratanadecho, P., Aoki, K. and Akahori, M. (2001). Experimental and numerical study of microwave drying in unsaturated porous material, Int. Comm. Heat Mass Transfer, Vol. 28 (5), pp. 605-616.
3. Ratanadecho, P., Aoki, K. and Akahori, M. (2002). Influence of irradiation time, particle sizes, and initial moisture content during microwave drying of multi-layered capillary porous materials, J. Heat Transfer, Vol. 124, February 2002, pp.151-161.
4. Sandua, C. (1986). Infrared radiative drying in food engineering: a process analysis, Biotechnology Progress, 2(3), pp. 109-119.
5. Nowak, D. and Lewicki, P.P. (2004). Infrared drying of apple slices, Innovative Food Science & Emerging Techonologies, Vol. 5, pp. 353-360.
6. Chaktranond, C., Jiamjiroch, K. and Ratanadecho, P. (2007). Influence of Electrohydrodymics (EHD) on heat and mass transfer in unsaturated Porous media, paper presented in the 21st Conference of Mechanical Engineering Network of Thailand 2007 (ME-NETT 21), Chonburi, Thailand.
7. Sakai, N. and Hanzawa, T. (1994). Application and advances in infrared heating in Japan, Trends in Food Science and Technology, Vol. 5(11). pp. 357-362.